

ISSN 0253-9837  
CN 21-1601/O6



# Chinese Journal of Catalysis

www.cjcat.org

Volume 40 | Number 1 | January 2019



催  
化  
学  
报  
  
C  
H  
I  
N  
E  
S  
E  
J  
O  
U  
R  
N  
A  
L  
O  
F  
C  
A  
T  
A  
L  
Y  
S  
I  
S  
  
J  
a  
n  
u  
a  
r  
y  
2  
0  
1  
9  
V  
o  
l.  
4  
0  
N  
o.  
1  
p

科  
学  
出  
版  
社



Editors-in-Chief Can Li (李灿) Tao Zhang (张涛)  
Transaction of The Catalysis Society of China

## In This Issue



**Cover:** Xi's group controls the synthesis of the silk-like  $\text{FeS}_2/\text{NiS}_2$  hybrid nanocrystal. The material has rich interfaces and defects, which is beneficial to enhance its catalytic performance. The picture shows the flexible battery assembled by this catalyst and their promising application. Read more about the article behind the cover on pages 43–51.

**封面:** 席聘贤课题组控制合成了丝绸状纳米结构( $\text{FeS}_2/\text{NiS}_2$ )。该材料具有丰富的界面和缺陷,有利于提升其催化性能。见本期第43–51页。

## About the Journal

*Chinese Journal of Catalysis* is an international journal published monthly by Chinese Chemical Society, Dalian Institute of Chemical Physics, Chinese Academy of Sciences, and Elsevier. The journal publishes original, rigorous, and scholarly contributions in the fields of heterogeneous and homogeneous catalysis in English or in both English and Chinese. The scope of the journal includes:

- ◆ New trends in catalysis for applications in energy production, environmental protection, and production of new materials, petroleum chemicals, and fine chemicals;
- ◆ Scientific foundation for the preparation and activation of catalysts of commercial interest or their representative models;
- ◆ Spectroscopic methods for structural characterization, especially methods for in situ characterization;
- ◆ New theoretical methods of potential practical interest and impact in the science and applications of catalysis and catalytic reaction;
- ◆ Relationship between homogeneous and heterogeneous catalysis;
- ◆ Theoretical studies on the structure and reactivity of catalysts.
- ◆ The journal also accepts contributions dealing with photo-catalysis, bio-catalysis, and surface science and chemical kinetics issues related to catalysis.

### Types of Contributions

- **Reviews** deal with topics of current interest in the areas covered by this journal. Reviews are surveys, with entire, systematic, and important information, of recent progress in important topics of catalysis. Rather than an assemblage of detailed information or a complete literature survey, a critically selected treatment of the material is desired. Unsolved problems and possible developments should also be discussed. Authors should have published articles in the field. Reviews should have more than 80 references.
- **Communications** rapidly report studies with significant innovation and major academic value. They are limited to four Journal pages. After publication, their full-text papers can also be submitted to this or other journals.
- **Articles** are original full-text reports on innovative, systematic and completed research on catalysis.
- **Highlights** describe and comment on very important new results in the original research of a third person with a view to highlight their significance. The results should be presented clearly and concisely without the comprehensive details required for an original article.
- **Perspectives** are short reviews of recent developments in an established or developing topical field. The authors should offer a critical assessment of the trend of the field, rather than a summary of literatures.
- **Viewpoints** describe the results of original research in general in some area, with a view to highlighting the progress, analyzing the major problems, and commenting the possible research target and direction in the future.

### Impact Factor

2017 SCI Impact Factor: **3.525**  
2017 SCI 5-Year Impact Factor: 2.736

### Abstracting and Indexing

Abstract Journals (VINITI)  
Cambridge Scientific Abstracts (CIG)  
Catalysts & Catalysed Reactions (RSC)  
Current Contents/Engineering, Computing and Technology  
(Clarivate Analytics ISI)  
Chemical Abstract Service/SciFinder (CAS)  
Chemistry Citation Index (Clarivate Analytics ISI)  
Japan Information Center of Science and Technology  
Journal Citation Reports/Science Edition (Clarivate Analytics ISI)  
Science Citation Index Expanded (Clarivate Analytics ISI)  
SCOPUS (Elsevier)  
Web of Science (Clarivate Analytics ISI)

### The Fifth Editorial Board of *Chinese Journal of Catalysis*

#### 《催化学报》第五届编辑委员会

**Publication** Monthly (12 issues)

**Started** in March 1980

Transaction of The Catalysis Society of China

**Superintended by**

Chinese Academy of Sciences (CAS)

**Sponsored by**

Chinese Chemical Society and Dalian  
Institute of Chemical Physics, CAS

**Editors-in-Chief** Can Li, Tao Zhang

**Edited by** Editorial Board of

*Chinese Journal of Catalysis*

Tel.: +86-411-84379240

E-mail: cjccatal@dicp.ac.cn

Add.: Dalian Institute of Chemical

Physics, CAS, 457 Zhongshan Road,

Dalian 116023, Liaoning, China

**Published by** Science Press

**Distributed by** Science Press,

16 Donghuangchengen North Street, Beijing

100717, China, Tel: +86-10-64017032

E-mail: sales\_journal@mail.sciencep.com

**Subscription Agents**

**Domestic** All Local Post Offices in China

**Foreign** China International Book Trading

Corporation, P.O.Box 399, Beijing 100044,

China

**Printed by**

Dalian Haida Printing Company, Limited

**Price** \$60

月刊 SCI收录 1980年3月创刊

中国化学会催化学会会刊

主管 中国科学院

主办 中国化学会

中国科学院大连化学物理研究所

主编 李灿 张涛

编辑 《催化学报》编辑委员会

出版 科学出版社

编辑部联系方式:

地址: 大连市沙河口区中山路 457 号

中国科学院大连化学物理研究所

邮编: 116023

电话: (0411)84379240

传真: (0411)84379543

电子信箱: cjccatal@dicp.ac.cn

国内统一连续出版物号 CN 21-1601/O6

国际标准连续出版物号 ISSN 0253-9837

CODEN THHPD3

广告经营许可证号 2013003

总发行 科学出版社

北京东黄城根北街16号, 邮编: 100717

电话: (010) 64017032

E-mail: sales\_journal@mail.sciencep.com

国内订购 全国各地邮政局

邮发代号 8-93

国外订购 中国国际图书贸易总公司

北京399信箱 邮编 100044

国外发行代号 M417

印刷 大连海大印刷有限公司

定价 60元

公开发行

#### Advisors (顾问)

Alexis T. Bell (美国)

Jürgen Caro (德国)

Gabriele Centi (意大利)

Michel Che (法国)

Yi Chen (陈懿)

Avelino Corma (西班牙)

Zi Gao (高滋)

Masatake Haruta (日本)

Mingyuan He (何鸣元)

Graham J. Hutchings (英国)

Johannes A. Lercher (德国)

S. Ted. Oyama (日本)

Daniel E. Resasco (美国)

Rutger A. van Santen (荷兰)

Ferdi Schüth (德国)

Huilin Wan (万惠霖)

Youchang Xie (谢有畅)

Qin Xin (辛勤)

Xiaoming Zheng (郑小明)

#### Editors-in-Chief (主编)

Can Li (李灿)

Tao Zhang (张涛)

#### Associate Editors (副主编)

Xingwei Li (李兴伟)

Haichao Liu (刘海超)

Roel Prins (瑞士)

Junwang Tang (唐军旺, 英国)

Peng Wu (吴鹏)

Qihua Yang (杨启华)

#### Members (编委)

Xinhe Bao (包信和)

Yong Cao (曹勇)

De Chen (陈德, 挪威)

Jingguang G. Chen (陈经广, 美国)

Weiping Ding (丁维平)

Yunjie Ding (丁云杰)

Xianzhi Fu (付贤智)

Naijia Guan (关乃佳)

Xinwen Guo (郭新闻)

Hongxian Han (韩洪宪)

Heyong He (贺鹤勇)

Hong He (贺泓)

Emiel J. M. Hensen (荷兰)

Jiahui Huang (黄家辉)

George W. Huber (美国)

Huanwang Jing (景欢旺)

Alexander Katz (美国)

Jinlin Li (李金林)

Jun Li (李隽)

Junhua Li (李俊华)

Weixue Li (李微雪)

Yingwei Li (李映伟)

Yongdan Li (李永丹)

Changjun Liu (刘昌俊)

Jingyue Liu (刘景月, 美国)

Zhongmin Liu (刘中民)

An-Hui Lu (陆安慧)

Marcel Schlaf (加拿大)

Susannah L. Scott (美国)

Jianyi Shen (沈俭一)

Wenjie Shen (申文杰)

Chunshan Song (宋春山, 美国)

Baolian Su (苏宝连, 比利时)

Dangsheng Su (苏党生)

Zhiyong Tang (唐智勇)

Zhijian Tian (田志坚)

Ying Wan (万颖)

Aiqin Wang (王爱琴)

Dezheng Wang (王德峥)

Feng Wang (王峰)

Jianguo Wang (王建国)

Ye Wang (王野)

Yong Wang (王勇, 美国)

Yingxu Wei (魏迎旭)

Zidong Wei (魏子栋)

Zili Wu (吴自力, 美国)

Chungu Xia (夏春谷)

Fengshou Xiao (肖丰收)

Jianliang Xiao (肖建良, 英国)

Zaiku Xie (谢在库)

Boqing Xu (徐柏庆)

Jie Xu (徐杰)

Longya Xu (徐龙伢)

Yushan Yan (严玉山, 美国)

Weimin Yang (杨为民)

Weishen Yang (杨维慎)

Shuangfeng Yin (尹双凤)

Jiaguoyu (余家国)

Youzhu Yuan (袁友珠)

Zongchao Zhang (张宗超)

Huijun Zhao (赵惠军, 澳大利亚)

Zhen Zhao (赵震)

Xiao-Dong Zhou (周晓东, 美国)

Yonggui Zhou (周永贵)

#### Young Members (青年编委)

Bingyang Bai (拜冰阳)

Shaowen Cao (曹少文)

Weili Dai (戴卫理)

Jiguang Deng (邓积光)

Yong Ding (丁勇)

Fan Dong (董帆)

Pingwu Du (杜平武)

Fengtao Fan (范峰滔)

Yanlong Gu (顾彦龙)

Yanqiang Huang (黄延强)

Changzhi Li (李昌志)

Fei Li (李斐)

Rengui Li (李仁贵)

Xiang Li (李翔)

Xin Li (李鑫)

Zhenxing Liang (梁振兴)

Gang Liu (刘钢)

Gang Liu (刘岗)

Mingce Long (龙明策)

Kangle Lv (吕康乐)

Botao Qiao (乔波涛)

Yong Qin (覃勇)

Feng Shi (石峰)

Wei Sun (孙伟)

Guoxiong Wang (汪国雄)

Xiuli Wang (王秀丽)

Yujie Xiong (熊宇杰)

Fan Yang (杨帆)

Hengquan Yang (杨恒权)

Changlin Yu (余长林)

Huogen Yu (余火根)

Yunbo Yu (余运波)

Wangcheng Zhan (詹望成)

Jing Zhang (张静)

Wenzhen Zhang (张文珍)

Liangshu Zhong (钟良枢)

Online Submission <https://mc03.manuscriptcentral.com/cjccatal>, <http://www.elsevier.com/locate/chnjc>

Homepage <http://www.cjccatal.org>, <http://www.journals.elsevier.com/chinese-journal-of-catalysis>



available at [www.sciencedirect.com](http://www.sciencedirect.com)



journal homepage: [www.elsevier.com/locate/chnjc](http://www.elsevier.com/locate/chnjc)



## Chinese Journal of Catalysis Graphical Contents

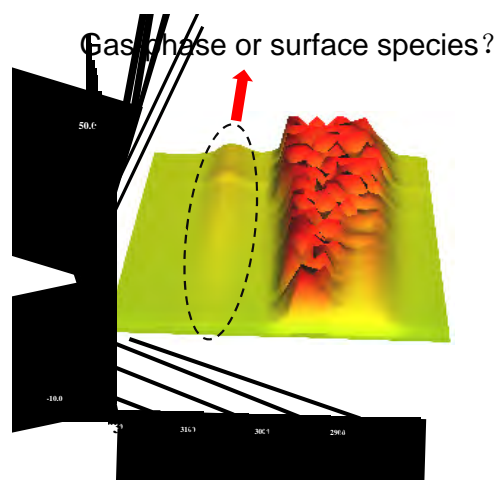
### Academic discussion

*Chin. J. Catal.*, 2019, 40: 1–3 doi: 10.1016/S1872-2067(18)63188-2

Comment On the correction of gas-phase signals during IR operando analyses

Frederic Meunier \*

*Institut de Recherches sur la Catalyse et l'Environnement, France*



The accuracy of dual beam Fourier transform infrared (DB-FTIR) spectrometer in eliminating the interference of gas-phase molecular vibration in gas/solid heterogeneous catalysis under reaction conditions is discussed.

### Reviews

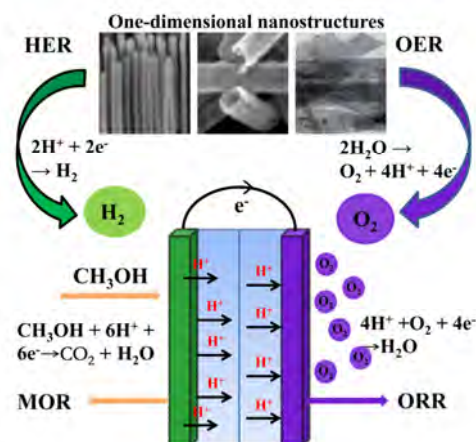
*Chin. J. Catal.*, 2019, 40: 4–22 doi: 10.1016/S1872-2067(18)63177-8

#### Recent advances in one-dimensional nanostructures for energy electrocatalysis

Ping Li, Wei Chen \*

*Changchun Institution of Applied Chemistry, Chinese Academic of Science; University of Science and Technology of China*

This overview summarizes the recent advances in one-dimensional metal nanostructures for energy electrocatalysis, including the main reactions in direct methanol fuel cells and water splitting.

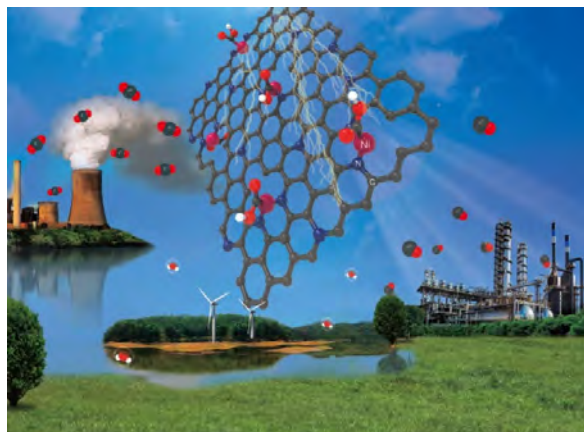


*Chin. J. Catal.*, 2019, 40: 23–37 doi: 10.1016/S1872-2067(18)63161-4

### Transition metal-nitrogen sites for electrochemical carbon dioxide reduction reaction

Chengcheng Yan, Long Lin, Guoxiong Wang\*, Xinxin Bao\*  
*Dalian Institute of Chemical Physics, Chinese Academy of Sciences;  
 University of Chinese Academy of Sciences*

Metal-nitrogen sites constituted of earth abundant elements with maximum atom-utilization efficiency have emerged as promising catalysts for electrochemical CO<sub>2</sub> reduction reaction.



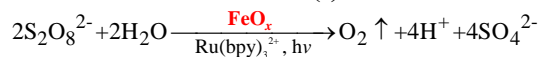
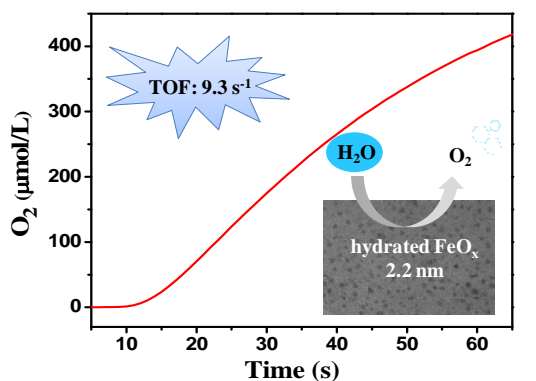
## Communication

*Chin. J. Catal.*, 2019, 40: 38–42 doi: 10.1016/S1872-2067(18)63190-0

### A hydrated amorphous iron oxide nanoparticle as active water oxidation catalyst

Zheng Chen, Qinge Huang, Baokun Huang, Fuxiang Zhang\*, Can Li\*  
*Dalian Institute of Chemical Physics, Chinese Academy of Sciences*

A hydrated amorphous iron oxide nanoparticle exhibits high water oxidation activity with TOF of 9.3 s<sup>-1</sup> in the photocatalytic Ru(bpy)<sub>3</sub><sup>2+</sup>-Na<sub>2</sub>S<sub>2</sub>O<sub>8</sub>.

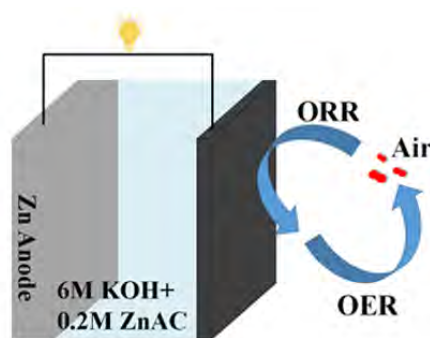
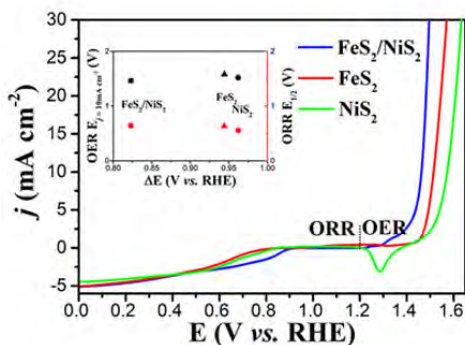


## Articles

*Chin. J. Catal.*, 2019, 40: 43–51 doi: 10.1016/S1872-2067(18)63175-4

### Synthesis of silk-like FeS<sub>2</sub>/NiS<sub>2</sub> hybrid nanocrystals with improved reversible oxygen catalytic performance in a Zn-air battery

Jing Jin, Jie Yin, Pinxian Xi\*  
*Lanzhou University*



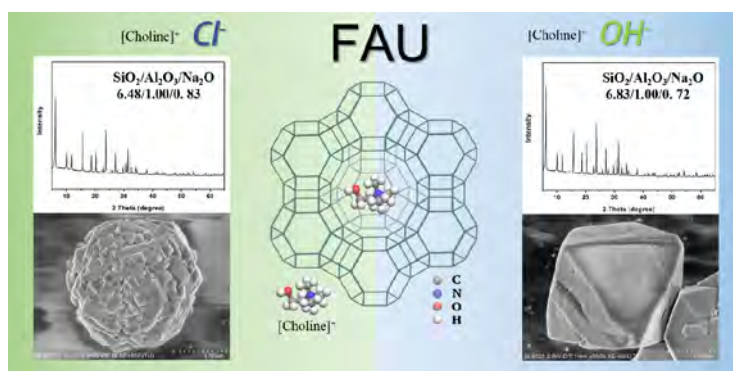
Herein, an efficient liquid exfoliation strategy was designed for producing silk-like FeS<sub>2</sub>/NiS<sub>2</sub> hybrid nanocrystals with enhanced reversible oxygen catalytic performance that displayed excellent properties for Zn-air batteries.

*Chin. J. Catal.*, 2019, 40: 52–59 doi: 10.1016/S1872-2067(18)63167-5

### Eco-friendly synthesis of high silica zeolite Y with choline as green and innocent structure-directing agent

Dawei He, Danhua Yuan, Zhijia Song, Yunpeng Xu \*, Zhongmin Liu \*

*Dalian Institute of Chemical Physics, Chinese Academy of Sciences; University of Chinese Academy of Sciences*



Choline chloride or choline hydroxide was used as an eco-friendly and nontoxic organic structure-directing agent (OSDA) for the synthesis of high silica zeolite Y with  $\text{SiO}_2/\text{Al}_2\text{O}_3$  ratios of 6.5–6.8.

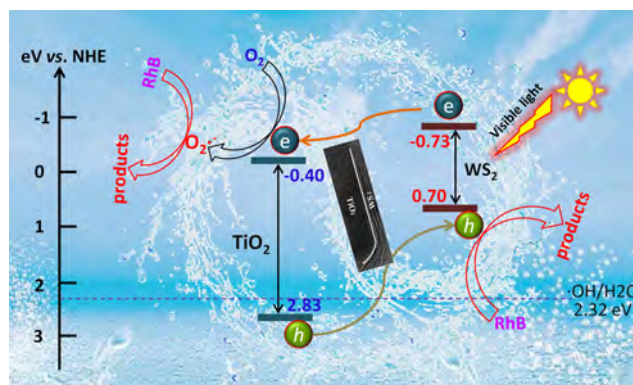
*Chin. J. Catal.*, 2019, 40: 60–69 doi: 10.1016/S1872-2067(18)63170-5

### Construction of 2D-2D $\text{TiO}_2$ nanosheet/layered $\text{WS}_2$ heterojunctions with enhanced visible-light-responsive photocatalytic activity

Yongchuan Wu, Zhongmin liu, Yaru Li, Jitao Chen, Xixi Zhu, Ping Na \*

*Tianjin University; College of Chemistry and Chemical Engineering; Shandong University of Science and Technology*

The 2D-2D TNS/ $\text{WS}_2$  heterojunction was successfully constructed by in-situ growing the layered  $\text{WS}_2$  on the surface of  $\text{TiO}_2$  nanosheet. The 2D-2D nanointerfaces boosted the separation of photogenerated carriers, thereby resulting in a higher photocatalytic activity.

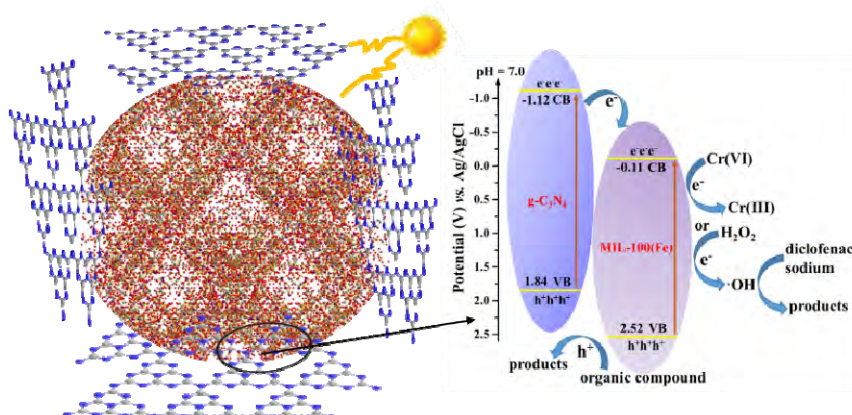


*Chin. J. Catal.*, 2019, 40: 70–79 doi: 10.1016/S1872-2067(18)63160-2

### Enhanced photocatalytic Cr(VI) reduction and diclofenac sodium degradation under simulated sunlight irradiation over MIL-100(Fe)/g- $\text{C}_3\text{N}_4$ heterojunctions

Xuedong Du, Xiaohong Yi, Peng Wang, Jiguang Deng \*, Chong-chen Wang \*

*Beijing University of Civil Engineering and Architecture; Beijing University of Technology*

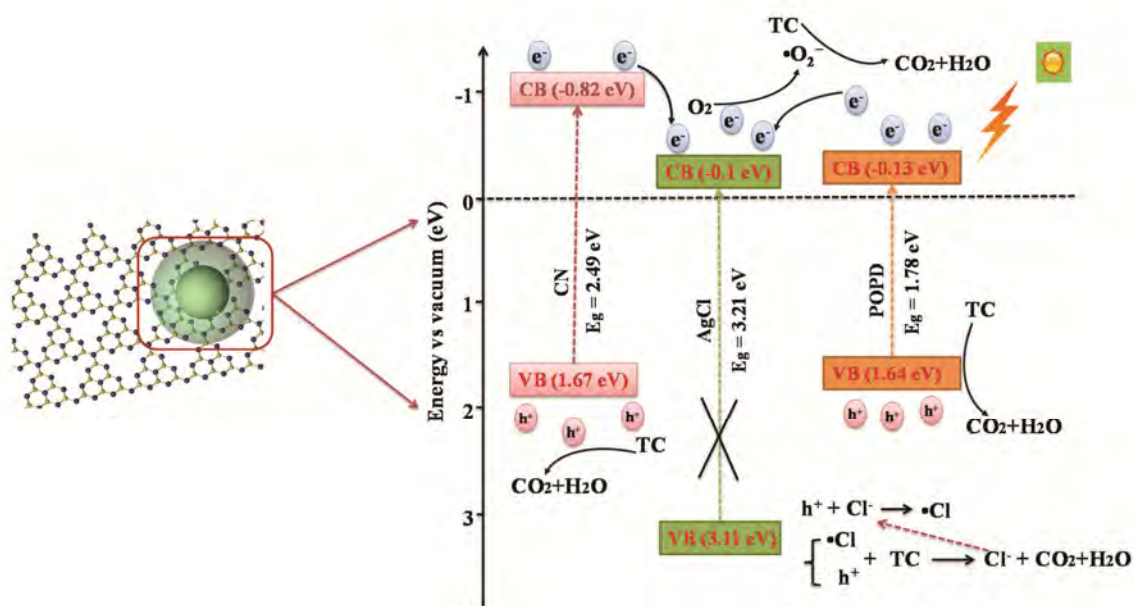


The MIL-100(Fe)/g- $\text{C}_3\text{N}_4$  hybrids show high photocatalytic activity under simulated sunlight and can reduce Cr(VI) to Cr(III) and decompose diclofenac sodium effectively.

*Chin. J. Catal.*, 2019, 40: 80–94 doi: 10.1016/S1872-2067(18)63172-9

### Fast electron transfer and enhanced visible light photocatalytic activity by using poly-o-phenylenediamine-modified AgCl/g-C<sub>3</sub>N<sub>4</sub> nanosheets

Linlin Sun, Chongyang Liu, Jinze Li, Yaju Zhou, Huiqin Wang \*, Pengwei Huo \*, Changchang Ma, Yongsheng Yan  
*Jiangsu University*

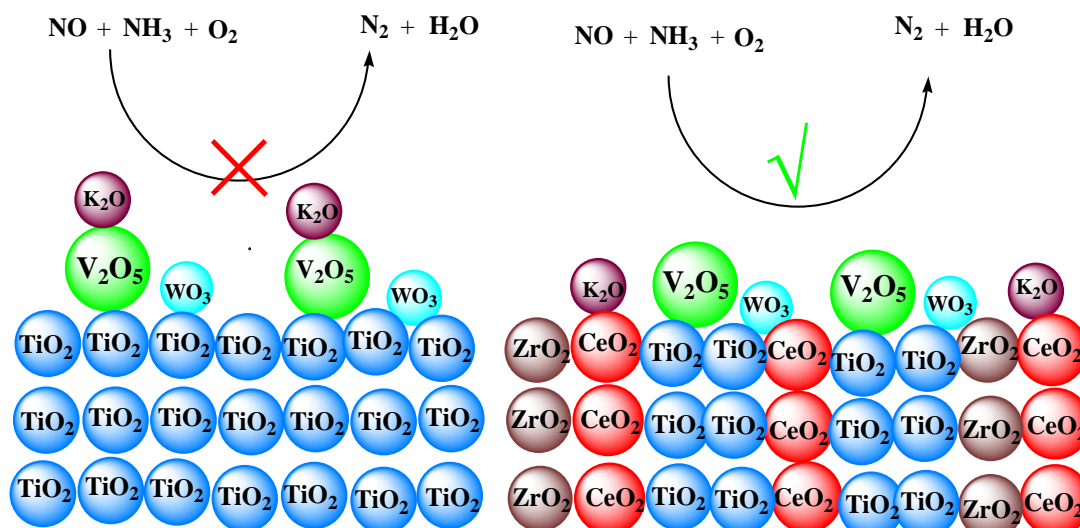


The degradation efficiency of tetracycline over PoPD/AgCl/CN composites synthesized by precipitation reaction and photoinitiated polymerization approach was three times higher than that over pure CN;  $\cdot\text{O}_2^-$  and  $\text{h}^+$  are the main reactive species in the case of PoPD/AgCl/CN.

*Chin. J. Catal.*, 2019, 40: 95–104 doi: 10.1016/S1872-2067(18)63184-5

### Improving the denitration performance and K-poisoning resistance of the V<sub>2</sub>O<sub>5</sub>-WO<sub>3</sub>/TiO<sub>2</sub> catalyst by Ce<sup>4+</sup> and Zr<sup>4+</sup> co-doping

Jun Cao, Xiaojiang Yao \*, Fumo Yang, Li Chen, Min Fu \*, Changjin Tang, Lin Dong  
*Chongqing Technology and Business University; Chongqing Institute of Green and Intelligent Technology, Chinese Academy of Sciences; Sichuan University; Nanjing University*



Co-doping of Ce<sup>4+</sup> and Zr<sup>4+</sup> enhances the denitration performance and K-poisoning resistance of V<sub>2</sub>O<sub>5</sub>-WO<sub>3</sub>/TiO<sub>2</sub> catalyst because more K atoms can be combined with Ce<sup>4+</sup> to yield the better protection of active vanadium species.

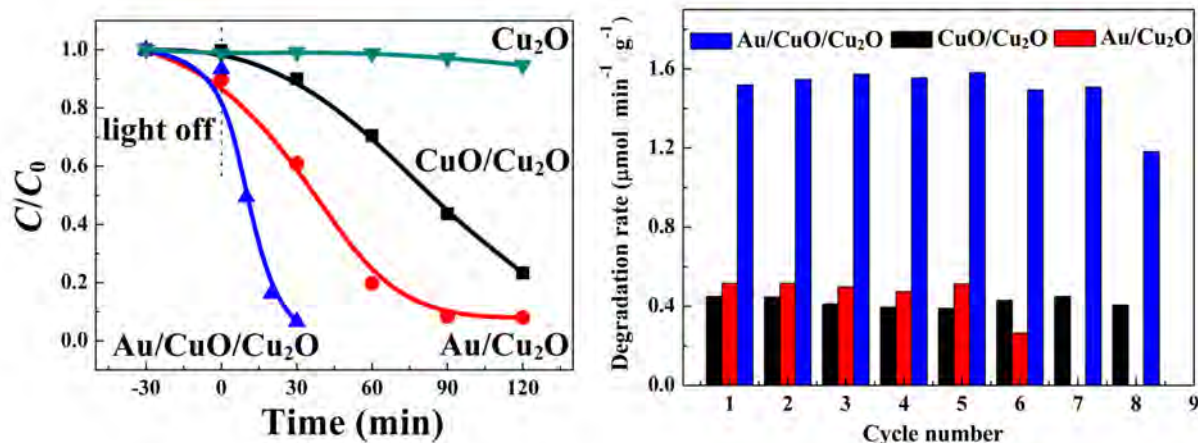
*Chin. J. Catal.*, 2019, 40: 105–113 doi: 10.1016/S1872-2067(18)63164-X

### Synergistic effects of CuO and Au nanodomains on Cu<sub>2</sub>O cubes for improving photocatalytic activity and stability

Denghui Jiang, Yuegang Zhang, Xinheng Li\*

Lanzhou Institute of Chemical Physics (LICP), Chinese Academy of Sciences; Central South University;

Suzhou Institute of Nano-tech and Nano-bionics, Chinese Academy of Sciences



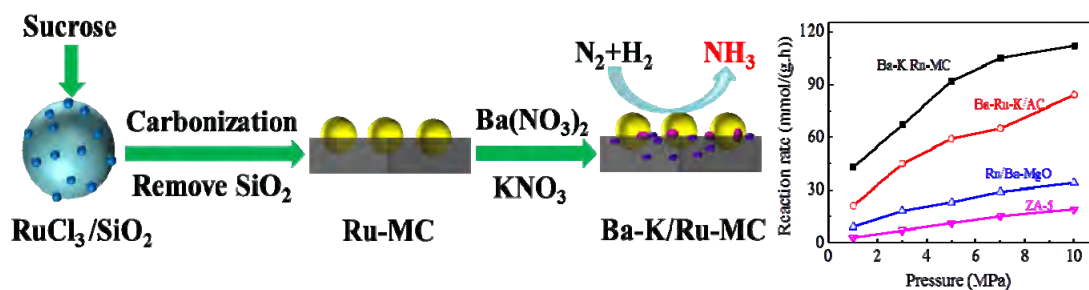
$\text{Au}/\text{CuO}/\text{Cu}_2\text{O}$  catalysts were synthesized by sequential surface oxidative and reductive deposition on  $\text{Cu}_2\text{O}$  surfaces improving both the photocatalytic activity and stability of  $\text{Cu}_2\text{O}$ .

*Chin. J. Catal.*, 2019, 40: 114–123 doi: 10.1016/S1872-2067(18)63192-4

### A highly stable and active mesoporous ruthenium catalyst for ammonia synthesis prepared by a $\text{RuCl}_3/\text{SiO}_2$ -templated approach

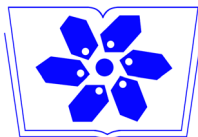
Yaping Zhou, Yongcheng Ma, Guojun Lan, Haodong Tang, Wenfeng Han, Huazhang Liu, Ying Li\*

Zhejiang University of Technology; Sichuan Huadi Construction Engineering Co., Ltd.



Semi-embedded  $\text{Ru-MC}$  has stable  $\text{Ru}$  NPs and strong interaction between  $\text{Ru}$  and  $\text{C}$  that promote the catalytic performance for ammonia synthesis.





中国科学院科学出版基金资助出版

月刊 SCI收录 2019年1月 第40卷 第1期



## 目次

### 学术讨论

- 1  
关于双光束红外光谱在气固相多相催化反应实时原位表征中气相校正的讨论  
Frederic Meunier

### 综述

- 4  
一维纳米材料在能源电催化中的研究进展  
李芊, 陈卫

- 23  
过渡金属-氮活性位在二氧化碳电化学还原反应中的应用  
阎程程, 林龙, 汪国雄, 包信和

### 快讯

- 38  
水合状态的无定形氧化铁作为高效水氧化催化剂的研究  
陈政, 黄清娥, 黄保坤, 章福祥, 李灿

### 论文

- 43  
可逆氧催化性能提升的FeS<sub>2</sub>/NiS<sub>2</sub>纳米复合物的合成及其在锌空电池中的应用  
靳晶, 殷杰, 刘瀚文, 席聘贤

- 52  
以胆碱为绿色无毒有机结构导向剂合成高硅Y型分子筛  
贺大威, 袁丹华, 宋智甲, 徐云鹏, 刘中民

- 60  
构建2D-2D TiO<sub>2</sub>纳米片/层状WS<sub>2</sub>异质结用以增强可见光响应光催化活性  
吴勇川, 刘中敏, 李亚茹, 陈继涛, 祝熙熙, 那平

- 70  
模拟太阳光照射下MIL-100(Fe)/g-C<sub>3</sub>N<sub>4</sub>异质结光催化Cr(VI)还原和双氯芬酸钠降解  
杜雪冬, 衣晓虹, 王鹏, 邓积光, 王崇臣

- 80  
聚邻苯二胺修饰AgCl/g-C<sub>3</sub>N<sub>4</sub>纳米片复合光催化剂的制备及性能研究  
孙林林, 刘重阳, 李金择, 周亚举, 王会琴, 霍鹏伟, 马长畅, 闫永胜

- 95  
Ce<sup>4+</sup>, Zr<sup>4+</sup>共掺杂提高V<sub>2</sub>O<sub>5</sub>-WO<sub>3</sub>/TiO<sub>2</sub>催化剂脱硝性能及抗K中毒能力  
曹俊, 姚小江, 杨复沫, 陈丽, 傅敏, 汤常金, 董林

- 105  
CuO和Au纳米结构协同增强Cu<sub>2</sub>O立方体光催化活性和稳定性  
蒋登辉, 张跃钢, 李鑫恒

- 114  
以RuCl<sub>3</sub>/SiO<sub>2</sub>为模板制备的高性能镶嵌式钌基氨合成催化剂  
周亚萍, 马永承, 蓝国钧, 唐浩东, 韩文锋, 刘化章, 李璘

### 相关信息

- 124 《催化学报》第五届编辑委员会  
128 Guide for Authors  
135 《催化学报》作者指南

英文全文电子版(国际版)由Elsevier出版社在ScienceDirect上出版  
<http://www.sciencedirect.com/science/journal/18722067>  
<http://www.elsevier.com/locate/chnjc>  
[www.cjatal.org](http://www.cjatal.org)  
在线投审稿网址  
<https://mc03.manuscriptcentral.com/cjatal>



available at www.sciencedirect.com



journal homepage: www.elsevier.com/locate/chnjc



## Article

# Eco-friendly synthesis of high silica zeolite Y with choline as green and innocent structure-directing agent

Dawei He <sup>a,b,†</sup>, Danhua Yuan <sup>a,†</sup>, Zhijia Song <sup>a,b</sup>, Yunpeng Xu <sup>a,\*</sup>, Zhongmin Liu <sup>a,#</sup><sup>a</sup> National Engineering Laboratory for Methanol to Olefins, Dalian National Laboratory for Clean Energy, Dalian Institute of Chemical Physics, Chinese Academy of Sciences, Dalian 116023, Liaoning, China<sup>b</sup> University of Chinese Academy of Sciences, Beijing 100049, China

## ARTICLE INFO

## Article history:

Received 12 September 2018

Accepted 23 September 2018

Published 5 January 2019

## Keywords:

Zeolite synthesis

FAU zeolite

High silica

Green organic structure-directing agent

(Hydro)thermal stability

## ABSTRACT

Zeolite synthesis in contemporary chemical industries is predominantly conducted using organic structure-directing agents (OSDAs), which are chronically hazardous to humans and the environment. It is a growing trend to develop an eco-friendly and nuisanceless OSDA for zeolite synthesis. Herein, choline is employed as a non-toxic and green OSDA to synthesize high silica Y zeolite with SiO<sub>2</sub>/Al<sub>2</sub>O<sub>3</sub> ratios of 6.5–6.8. The prepared Y zeolite samples exhibited outstanding (hydro)thermal stability at ultrahigh temperature owing to the higher SiO<sub>2</sub>/Al<sub>2</sub>O<sub>3</sub> ratio. The XRF, SEM, <sup>29</sup>Si-NMR and <sup>13</sup>Na+ results suggested that choline plays a structure-directing role in the synthesis of Y zeolite, while the feed molar fraction of Na<sup>+</sup> is a crucial determinant for the framework SiO<sub>2</sub>/Al<sub>2</sub>O<sub>3</sub> ratio and the crystal morphology.

© 2019, Dalian Institute of Chemical Physics, Chinese Academy of Sciences.

Published by Elsevier B.V. All rights reserved.

## 1. Introduction

Zeolites have been extensively used as catalysts, adsorbents and ion-exchangers owing to their well-defined microporous structures, adjustable acidities and a large variety of available frameworks and chemical compositions [1–5]. Among the approximate reported 230 zeolite framework types, the vast majority of zeolites are synthesized in the presence of organic structure-directing agents (OSDAs), and more novel topologies are synthesized by the application of new OSDAs [6–8]. On the other hand, most common organic templates are quaternary ammonium or amines, which are usually unavailable or toxic or environmentally hazardous. Therefore, it is desirable to develop eco-friendly synthesis routes with the use of non-toxic and green OSDAs [9–11]. For example, polyquaternium-6, a typical

component of shampoo, was successfully used as a template to synthesize EMT-rich faujasite, which offers the possibility of industrial applications of EMT zeolites [12]. However, it has been demonstrated that among a huge amount of organics, only a small minority of organics have the ability as structure-directing agents for zeolite synthesis. It is more difficult to find a non-toxic and eco-friendly OSDA with “fitting” size and shape for the targeted zeolite topology.

Herein we focus on the synthesis of Y zeolite with a 12-membered window size of 7.4 Å and a supercage cavity size of 12 Å, which has been vastly used as the main active component of fluidized catalytic cracking (FCC) catalysts so far [13–18]. It has been demonstrated that increasing the framework SiO<sub>2</sub>/Al<sub>2</sub>O<sub>3</sub> ratio of Y zeolite is helpful to enhance its acid strength, (hydro)thermal stability and catalytic activity [19,20].

<sup>†</sup> These authors contributed equally to this work.

\* Corresponding author. Tel: +86-411-84379518; Fax: +86-411-84379038; E-mail: xuyy@dicp.ac.cn

# Corresponding author. Tel: +86-411-84379998; Fax: +86-411-84379038; E-mail: liuzm@dicp.ac.cn

DOI: 10.1016/S1872-2067(18)63167-5 | http://www.sciencedirect.com/science/journal/18722067 | Chin. J. Catal., Vol. 40, No. 1, January 2019

Whereas there has been a restricted upper limit for the  $\text{SiO}_2/\text{Al}_2\text{O}_3$  ratio of Y zeolite prepared by traditional OSDA-free synthesis routes [21]. Nowadays, the most widely employed zeolite Y in industry is ultra-stable zeolite Y (or USY,  $\text{SiO}_2/\text{Al}_2\text{O}_3$  ratio > 5) prepared by post-treatments to remove framework aluminium [22]. The post-synthesis treatments include hydrothermal dealumination and treatment with chemicals, which cause environmental pollution and high energy consumption, and compromise the structural integrity of zeolite, owing to reduplicative calcination and chemical treatments [23–26]. Compared with these post-treatments, one-step direct synthesis methods in the presence of OSDAs are beneficial for the synthesis of high silica Y zeolite with higher crystallinity and avoid lots of complicated physicochemical treatments.

Delprato et al. [27] firstly developed a one-step direct synthesis method for zeolite Y with  $\text{SiO}_2/\text{Al}_2\text{O}_3$  ratio of around 9 by employing crown ether (15-crown-5) as an OSDA in 1990. Inspired by crown ether, polyethylene oxides and tris(3,6-dioxahexyl)amine, which are acyclic molecules containing  $-\text{OCH}_2\text{CH}_2-$  groups similar to crown ether, were successfully used to synthesize zeolite Y ( $\text{SiO}_2/\text{Al}_2\text{O}_3$  ratio = 6–7) [28]. In 2015, Xiao et al. [29] studied quaternary ammonium salts and synthesized high silica zeolite Y in the presence of *N*-methylpyridinium iodide. Our group used ethyl(or butyl)-3-methylimidazolium bromide and tetraethylammonium hydroxide as OSDAs for the synthesis of high silica zeolite Y [30,31]. Nevertheless, the above OSDAs, especially crown ether, are expensive, toxic and environmentally unfriendly, which are unavailable for wide use in petrochemical processes. The development of an eco-friendly and “fitting” OSDA is difficult yet imperative to fill the gap in the synthesis of Y zeolite with the use of OSDAs.

Herein we focus on choline, a nontoxic, green and low-cost OSDA. Choline is a water-soluble vitamin-like essential nutrient that refers to quaternary ammonium salt containing *N,N,N*-trimethylethanolammonium cation. Choline was first isolated by Adolph Strecker from animal bile [32]. Nowadays, choline is industrially produced at a few thousand tons per year by 100% atom economy process [33]. Choline has been employed as a structure-directing agent to synthesize zeolites such as ZSM-4, SSZ-13 and SAPO-5 [34–36]. In the present work, the synthetic methodology is rationally designed to use choline as an eco-friendly and nontoxic OSDA in the synthesis of high silica zeolite Y for the first time. The sample ChCl-Y is synthesized with choline chloride and ChOH-Y is prepared with choline hydroxide. They both show good crystallinity and high framework  $\text{SiO}_2/\text{Al}_2\text{O}_3$  ratio. By contrast, different properties of ChCl-Y and ChOH-Y reveal to us the separate roles and relationship of  $\text{Na}^+$  and OSDA<sup>+</sup> in the synthesis of high silica Y zeolite. Both the products ChCl-Y and ChOH-Y show more outstanding high temperature thermal and hydrothermal stability, compared with conventional zeolite Y. Given the huge amount of zeolite Y used worldwide as adsorbents and FCC catalysts, the ability to enhance the  $\text{SiO}_2/\text{Al}_2\text{O}_3$  ratio via the use of choline as an eco-friendly and economically viable OSDA would have a significant impact on the (petro)chemical industry and would be a great progress.

## 2. Experimental

### 2.1. ChCl-Y Preparation

Firstly, 3.41 g choline chloride ([choline]Cl, Aladdin Chemical), 2.00 g sodium metaaluminate ( $\text{NaAlO}_2$ , Sinopharm Chemical) and 1.95 g sodium hydroxide (NaOH, Sinopharm Chemical) were dissolved in 26.65 g deionized water and stirred until a clear solution. Next, 24.60 g of silica sol ( $\text{SiO}_2$  29.8% aq. solution, Qingdao Ocean Chemical) was added in the above clear solution with strong agitation. The final gel was prepared with molar composition of  $1.0\text{NaAlO}_2 : 5.0\text{SiO}_2 : 2.0\text{NaOH} : 1.0[\text{choline}]\text{Cl} : 100\text{H}_2\text{O}$ . The mixture was stirred for 12 h at ambient temperature and maintained in ovens at 110 °C for 10 d. Calcined sample ChCl-Y was obtained after calcination at 550 °C for 4 h.

### 2.2. ChOH-Y Preparation

Firstly, 6.60 g choline hydroxide ([choline]OH, 45% aq. solution, Acros Organics), 2.00 g  $\text{NaAlO}_2$  and 0.98 g NaOH were dissolved in 23.00 g deionized water with stirring to form a clear solution. Next, 24.60 g silica sol was mixed with the above solution with strong agitation for 12 h at ambient temperature. ChOH-Y was synthesized in stainless steel autoclaves at the crystallization temperature of 110 °C for 12 d, with molar composition of  $1.0\text{NaAlO}_2 : 5.0\text{SiO}_2 : 1.0\text{NaOH} : 1.0[\text{choline}]\text{OH} : 100\text{H}_2\text{O}$ . Calcined sample ChOH-Y was obtained after calcination at 550 °C for 4 h.

To investigate the role of choline in the synthesis of zeolite Y, the sample Na-Y was designed as a reference sample with a composition of  $1.0\text{NaAlO}_2 : 5.0\text{SiO}_2 : 2.2\text{NaOH} : 100\text{H}_2\text{O}$ . Na-Y sample was synthesized at 100 °C with a reaction time of 14 d.

### 2.3. Characterization of Zeolites

The X-ray diffraction (XRD) patterns were acquired using a PANalytical X'Pert PRO X-ray diffractometer using  $\text{Cu-K}\alpha$  radiation with  $\lambda = 1.54059 \text{ \AA}$ , operating at 40 kV and 40 mA. The samples were scanned at  $12^\circ/\text{min}$  between  $2\theta$  angles of  $5^\circ$ – $65^\circ$ . Scanning electron microscopy (SEM) images were collected with a Hitachi SU8020 scanning electron microscopy.  $\text{N}_2$  adsorption-desorption isotherms of the samples were measured at  $-196 \text{ }^\circ\text{C}$  on a Micromeritics ASAP 2020 system. The solid state  $^{29}\text{Si-NMR}$  and  $^{27}\text{Al-NMR}$  experiments were conducted on a Bruker AvanceIII spectrometer equipped with a 14.1 T wide-bore magnet. TG-DSC measurement was conducted on a TA Q-600 analyzer with a heating rate of  $10 \text{ }^\circ\text{C}/\text{min}$  from ambient temperature to  $1100 \text{ }^\circ\text{C}$  in an air flow of  $100 \text{ mL}/\text{min}$ . The organic elemental composition of samples was measured by elemental analysis on an Elementar vario EL cube elemental analyzer. The chemical composition of the samples was calculated with a Philips Magix-601 X-ray fluorescence (XRF) spectrometer. Inductively coupled plasma optical emission spectrometry (ICP-OES) analysis was conducted with a PerkinElmer 7300DV.

### 3. Results and discussion

#### 3.1. Results of ChCl-Y and ChOH-Y prepared with variational OH<sup>-</sup> concentrations

The XRD patterns of the as-synthesized products ChCl-Y and ChOH-Y are respectively shown in Fig. 1A and Fig. 1B. The X-ray diffraction peaks with a high intensity are in agreement with the typical topological features of theoretical FAU framework. It indicates that Y zeolites with good crystallinity are synthesized by employing [choline]Cl or [choline]OH as an OSDA. The crystal morphologies of ChCl-Y and ChOH-Y are entirely different in SEM micrographs (Figs. 1C, 1D and S1). ChOH-Y exhibits uniform cubic octahedral crystals, and ChCl-Y shows spherical agglomerates with superficial triangle cone. It is reported that the crystal morphologies are affected by some experimental factors, for examples, the species of structure-directing agents and the special silica source or aluminium source [37–39]. The relationship between the dramatically different morphologies and the crystallization curves of ChOH-Y and ChCl-Y has aroused our attention. The crystallization curves of ChCl-Y and ChOH-Y samples are presented in Fig. 1E and 1F wherein the relative crystallinity changes with various reaction time. The relative crystallinity is estimated by the reflection intensities of the X-ray diffraction peaks (1 1 1), (2 2 0) and (3 3 1) of the samples. Both the crystallization curves of ChCl-Y and ChOH-Y exhibit typical S-shaped curves, which indicate that the crystallization process of Y zeolite is comprised of induction period, continuous growth period and stable crystallization period. The induction period of ChOH-Y is 6 d, which is longer than that (4 d) of ChCl-Y. The crystallization of zeolite Y from ChOH-Y is completed within 12 d, which is also longer than that (9 d) of ChCl-Y. It is concluded that ChCl-Y has a faster generation rate and faster growth rate compared with ChOH-Y.

As the synthesis process and the composition of ChCl-Y and

ChOH-Y are shown above, ChCl-Y and ChOH-Y are designed with the same feed molar ratio of [choline]<sup>+</sup> and OH<sup>-</sup>. However, the sample ChCl-Y is synthesized with Na<sup>+</sup>/SiO<sub>2</sub> feed ratio of 0.6, which is higher than that of ChOH-Y (0.4) in the starting gels. Therefore it means that the change of Na<sup>+</sup> feed molar ratio has a major influence on zeolite morphologies and crystallization process. Na<sup>+</sup> is proposed to coordinate water molecular with subsequent displacement by silicate and aluminate species to form aluminosilicate microorganization, or further nucleation centers in the synthesis of zeolites. Therefore, higher Na<sup>+</sup> molar ratio of the starting gels contributes to shortening the crystallization time and improving the nucleation rate which trends to the agglomerates of small cubic octahedral crystal.

The N<sub>2</sub> adsorption-desorption isotherms of calcined and as-synthesized samples are respectively shown in Fig. 2A and Fig. 2B. Calcined samples ChCl-Y and ChOH-Y exhibit a typical type-I adsorption-desorption isotherm, indicating that they are mainly consisted of very uniform micropores. The BET specific surface area, *t*-plot micropore area and pore volume of the samples are listed in Table S1. The BET specific surface area of the calcined samples ChCl-Y and ChOH-Y are 735.2 and 730.7 m<sup>2</sup>/g, respectively, which are slightly larger than that (694.1 m<sup>2</sup>/g) of Na-Y. The *t*-plot micropore area of ChCl-Y and ChOH-Y are 679.0 and 675.9 m<sup>2</sup>/g, which indicates the presence of abundant micropores in the synthetic samples ChCl-Y and ChOH-Y. The large BET specific surface area and uniform micropore property demonstrated that the use of choline chloride and choline hydroxide is helpful to the formation of micropore structure.

As shown in Fig. 2A and Fig. 2B, BET specific surface area of the as-synthesized samples ChCl-Y and ChOH-Y is much smaller than that of calcined ChCl-Y and ChOH-Y accordingly. Clearly, as-synthesized ChCl-Y and ChOH-Y undergo minimal adsorption, suggesting that the microporous structure is occupied with an amount of organic template. As-synthesized ChCl-Y and

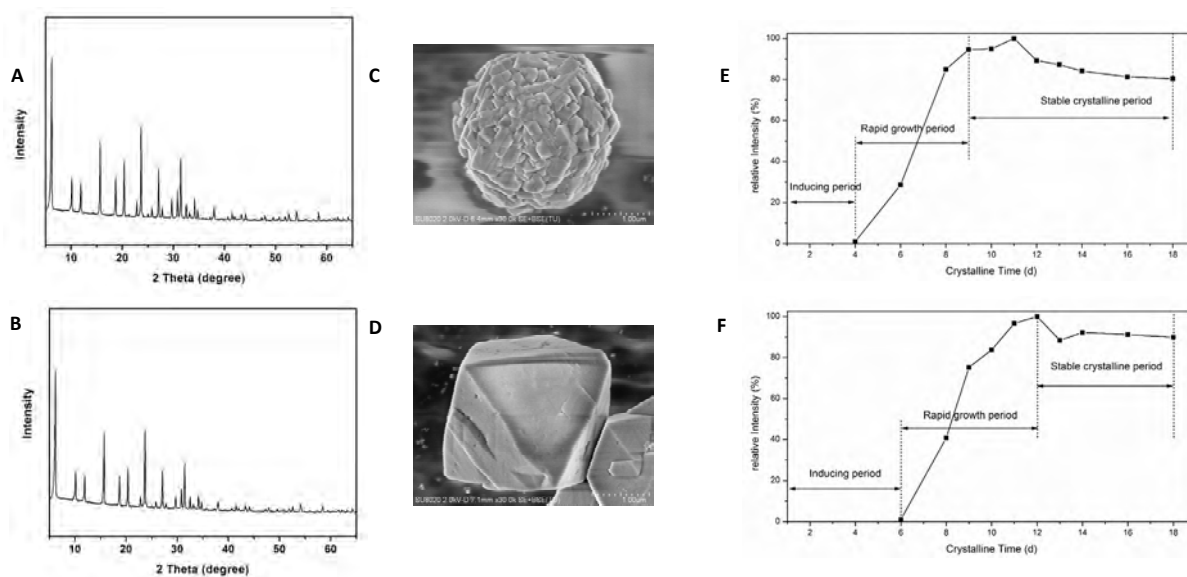


**Fig. 1.** XRD patterns of ChCl-Y (A) and ChOH-Y (B), SEM images of ChCl-Y (C) and ChOH-Y (D), and crystallization kinetic curves of ChCl-Y (E) and ChOH-Y (F).

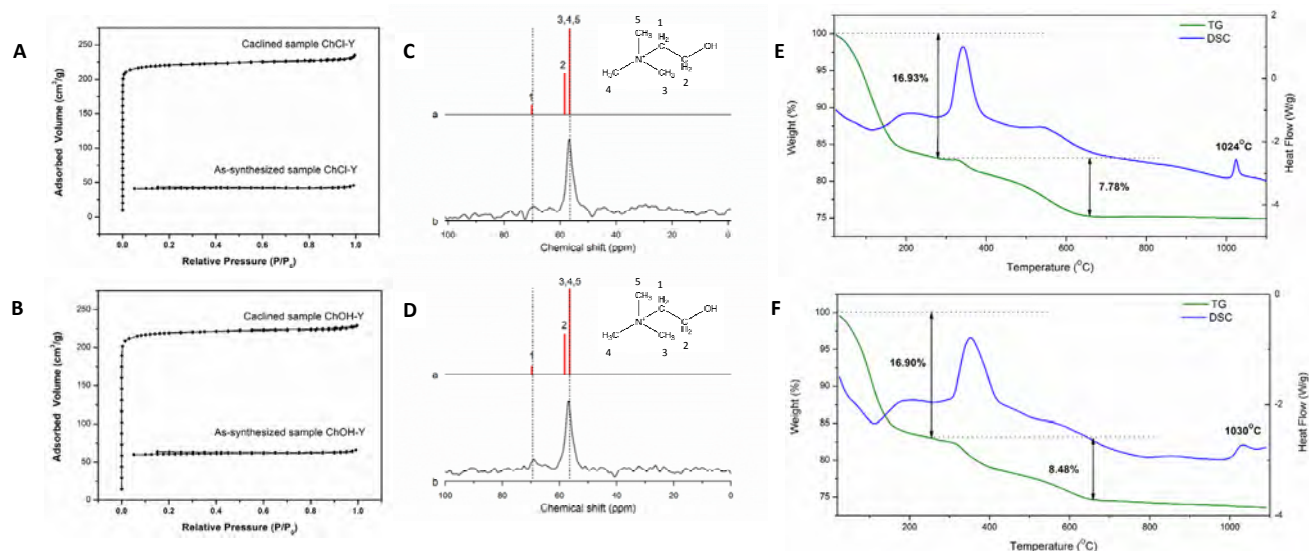


**Fig. 2.** N<sub>2</sub> adsorption-desorption isotherms of the as-synthesized and calcined ChCl-Y (A) and ChOH-Y (B), <sup>13</sup>C NMR spectra (C) of choline (a) and ChCl-Y (b), <sup>13</sup>C NMR spectra (D) of choline (a) and ChOH-Y (b), and TG/DSC curves of ChCl-Y (E) and ChOH-Y (F).

ChOH-Y samples exhibit a similar <sup>13</sup>C-NMR spectrum (Fig. 2C and Fig. 2D). There is a sharp peak appeared at 56.8 ppm in both <sup>13</sup>C NMR spectra, which is specifically assigned to methyl groups nearby nitrogen atom in choline molecular. The peak shift at 68 ppm is attributed to methoxy groups of choline. It is demonstrated that [choline]<sup>+</sup> acts as a structure-directing role in the synthesis of both ChCl-Y and ChOH-Y. The TG/DSC curves of as-synthesized ChCl-Y and ChOH-Y are shown in Fig. 2E and 2F. The TG/DSC results also prove that choline participates in the formulation of FAU framework as structure-directing agents. The endothermic weight loss at 100–300 °C is attributed to water desorption from samples. The water adsorption of ChCl-Y and ChOH-Y is respectively 16.93% and 16.90%. The weight loss accompanied by raised exothermic peaks at 300–650 °C in ChCl-Y and ChOH-Y is respectively 7.78% and 8.48%, which is attributed to the decomposition of organic templates. Carbon (C) and nitrogen (N) weight percentage of ChCl-Y and ChOH-Y is measured by elemental analysis (Table 1). The as-synthesized sample ChCl-Y contains 4.06 wt% carbon and 0.84 wt% nitrogen, which are obviously lower than 5.49 wt% carbon and 1.14 wt% nitrogen of ChOH-Y. The C/N molar ratios of both ChCl-Y and ChOH-Y are 5.6, close to that (5.0) of [choline]<sup>+</sup> (chemical formulae of [choline]<sup>+</sup>: C<sub>5</sub>H<sub>13</sub>OHN<sup>+</sup>). It is also a powerful evidence that [choline]<sup>+</sup> acts as a structure-directing agent in the synthesis of high silica Y. The elemental analysis results of Na-Y are set out in Table 1,

suggesting that the organic content of Na-Y is close to zero because Na-Y is synthesized without any organic template. In Table 1, the Na<sub>2</sub>O/Al<sub>2</sub>O<sub>3</sub> ratios of ChCl-Y and ChOH-Y are respectively 0.83 and 0.74, which are far smaller than that of Na-Y (0.98) by XRF data. The ICP calculation results exhibit that the Na<sub>2</sub>O/Al<sub>2</sub>O<sub>3</sub> ratios of ChCl-Y, ChOH-Y and Na-Y are respectively 0.83, 0.72 and 1.01, which are close to the XRF calculation. It is confirmed that [choline]<sup>+</sup> acts as a structuring-directing agent partially replacing Na<sup>+</sup> to occupy FAU supercages and compensate the negatively-charged Al framework sites. It is notable that carbon content of ChCl-Y is less than that of ChOH-Y and Na<sup>+</sup> content of ChCl-Y is higher than that of ChOH-Y in the contrary.

The <sup>27</sup>Al MAS-NMR and <sup>29</sup>Si MAS-NMR spectrograms of ChCl-Y, ChOH-Y and Na-Y samples are presented in Fig. 3. They show almost the same <sup>27</sup>Al MAS-NMR spectrograms with only a sharp and symmetric peak centered at about 60 ppm, which is identified as tetrahedrally-coordinated framework aluminum, implying that the samples contain no octahedrally-coordinated aluminium of extra framework. The <sup>29</sup>Si MAS-NMR spectra of high silica ChCl-Y and ChOH-Y show that the Si(2Al) peak is less intense but the Si(1Al) and Si(0Al) signals are more intense, compared to the corresponding signals of low silica Na-Y, wherein Si(*n*Al) represents that one Si atom connects to *n* Al atoms and (4–*n*) Si atoms in the second coordination shell by a bridging oxygen. The results indicate that choline as an OSDA

**Table 1**

The SiO<sub>2</sub>/Al<sub>2</sub>O<sub>3</sub> ratios and Na<sub>2</sub>O/Al<sub>2</sub>O<sub>3</sub> ratios obtained by XRF, <sup>29</sup>Si-NMR and ICP, and OSDA content of the as-synthesized products ChCl-Y, ChOH-Y, ChCl/ChOH:0.5/0.5-Y and Na-Y.

Sample	SiO <sub>2</sub> /Al <sub>2</sub> O <sub>3</sub> molar ratio			Na <sub>2</sub> O/Al <sub>2</sub> O <sub>3</sub> molar ratio		SDA content by elemental analysis		
	XRF	<sup>29</sup> Si-NMR	ICP	XRF	ICP	C (wt%)	N (wt%)	C/N ratio <sup>a</sup>
ChCl-Y	6.46	6.34	6.48	0.83	0.83	4.06	0.84	5.6
ChOH-Y	6.78	6.54	6.83	0.74	0.72	5.49	1.14	5.6
ChCl/ChOH:0.5/0.5-Y	6.56	6.46	6.67	0.79	0.77	5.11	1.07	5.6
Na-Y	5.56	5.40	5.50	0.98	1.01	0.24	0.07	—

<sup>a</sup> The molar ratio of carbon to nitrogen calculated by elemental analysis.

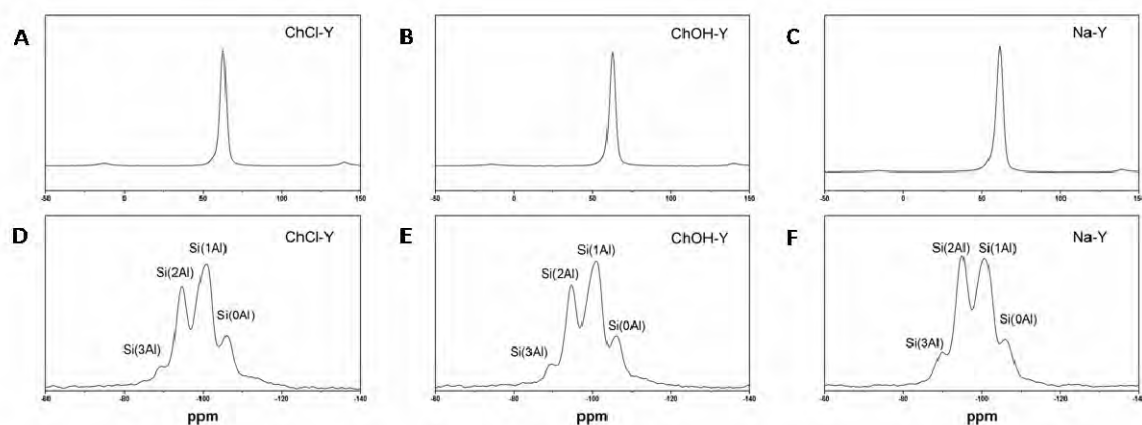


Fig. 3.  $^{27}\text{Al}$  MAS-NMR spectrograms of (A) ChCl-Y, (B) ChOH-Y and (C) Na-Y, and  $^{29}\text{Si}$  MAS-NMR spectrograms of (D) ChCl-Y, (E) ChOH-Y and (F) Na-Y.

could decrease the number of framework aluminium atoms per unit cell and increase the framework  $\text{SiO}_2/\text{Al}_2\text{O}_3$  ratio, which has been certified the calculation by XRF and ICP methods.

The  $\text{SiO}_2/\text{Al}_2\text{O}_3$  ratio of the three products ChOH-Y, ChCl-Y and Na-Y presented in Table 1 are calculated by XRF,  $^{29}\text{Si}$ -NMR and ICP. The XRF data indicate that ChCl-Y and ChOH-Y have higher  $\text{SiO}_2/\text{Al}_2\text{O}_3$  ratios of 6.46 and 6.78, which are much higher than that (5.56) of Na-Y zeolites with the traditional synthesis method. It could be explained by the theory that relatively larger organic cations ([choline] $^+$ ) with a lower charge density introduce a lower number of positive charges than small inorganic cations ( $\text{Na}^+$ ) within the zeolite cages, thus matching a lower number of framework Al atoms with negative charges, and increasing the framework  $\text{SiO}_2/\text{Al}_2\text{O}_3$  ratio. ChCl-Y and ChOH-Y have  $\text{SiO}_2/\text{Al}_2\text{O}_3$  ratios of 6.48 and 6.83 obtained by ICP analysis, which is in agreement with XRF calculation. The  $^{29}\text{Si}$  NMR spectroscopy is also used as an accurate characterization measuring the framework  $\text{SiO}_2/\text{Al}_2\text{O}_3$  ratio. The  $\text{SiO}_2/\text{Al}_2\text{O}_3$  ratios of the samples are calculated with the signals of  $\text{Si}(n\text{Al})$  species ( $n = 0-3$ ) in Fig. 3. The framework  $\text{SiO}_2/\text{Al}_2\text{O}_3$  ratios of ChCl-Y and ChOH-Y are respectively 6.34 and 6.54, whereas the  $\text{SiO}_2/\text{Al}_2\text{O}_3$  ratio of Na-Y is only 5.4, far below the framework  $\text{SiO}_2/\text{Al}_2\text{O}_3$  ratios of ChCl-Y and ChOH-Y. The  $^{29}\text{Si}$  NMR results are slightly lower than those obtained by XRF and ICP, which could be explained by the presence of partial Al sites substituted by terminal OH species in the framework, decreasing the data calculated by the  $^{29}\text{Si}$ -NMR spectrum. It is a great breakthrough that high silica zeolite Y could be synthesized with choline as a low-cost and eco-friendly organic template. Even more remarkable, ChOH-Y has a higher  $\text{SiO}_2/\text{Al}_2\text{O}_3$  ratio than ChCl-Y.

### 3.2. Synthesis design and characterization of ChCl/ChOH:0.5/0.5-Y and other samples

It arouses our interest that not only ChCl-Y and ChOH-Y exhibit entirely different crystal morphologies, but also the choice of choline chloride and choline hydroxide has a great influence on the framework  $\text{SiO}_2/\text{Al}_2\text{O}_3$  ratio. This gives us a brand new idea how to increase  $\text{SiO}_2/\text{Al}_2\text{O}_3$  ratio of Y zeolite, and impels us to further investigate the roles and relationship of [choline] $^+$

and  $\text{Na}^+$  in the synthesis of zeolite Y with OSDAs. As discussed in the previous part, the physicochemical differences of ChCl-Y and ChOH-Y are caused by the various feed molar ratio of  $\text{Na}^+$  in the starting gels. In general, alkali-metal cations ( $\text{Na}^+$ ) play two roles in the synthesis of zeolite, acting as (i) a source of alkalinity ( $\text{NaOH}$  is commonly used in Y zeolite synthesis) and (ii) a limited structure-directing agent [2]. [choline] $^+$  has been confirmed to be a structure-directing agent in the synthesis process of both ChCl-Y and ChOH-Y, but only choline hydroxide can be used as the source of alkalinity. Therefore choline hydroxide could provide sufficient alkalinity in the synthesis of ChOH-Y, use only half the amount of raw material  $\text{NaOH}$  during the synthesis of ChCl-Y, and sharply decrease the feedstock amount of  $\text{Na}^+$  (nearly one third). Based on the as $\text{Na}^+$ sumption that the differences of ChCl-Y and ChOH-Y are caused by the variation of  $\text{Na}^+$  feed ratio, a typical sample ChCl/ChOH:0.5/0.5-Y is designed with the  $\text{Na}^+/\text{SiO}_2$  feed molar ratio (0.5) between that of ChCl-Y (0.6) and ChOH-Y (0.4). The synthetic methodology is rationally designed with the same [choline] $^+$  and  $\text{OH}^-$  concentration as ChCl-Y and ChOH-Y by changing ChOH/ $\text{NaOH}$  ratio. The corresponding XRD pattern shows that ChCl/ChOH:0.5/0.5-Y has FAU topological structure with good crystallization (Fig. 4A). The SEM image (Fig. 4B) shows uniform irregular polyhedron, which is different with the morphology of both ChCl-Y and ChOH-Y. Therefore, the change of  $\text{Na}^+$  feed molar ratio has a decisive influence on the crystal morphology. Comparing the  $\text{SiO}_2/\text{Al}_2\text{O}_3$  ratio,  $\text{Na}_2\text{O}/\text{Al}_2\text{O}_3$  ratio and OSDA content in Table 1, it is obviously shown a regular variation of the final products: as the  $\text{Na}^+/\text{SiO}_2$  feed molar fraction (0.6, 0.5 and 0.4 corresponding to ChCl-Y, ChCl/ChOH:0.5/0.5-Y and ChOH-Y) in their starting gels reduces, the  $\text{SiO}_2/\text{Al}_2\text{O}_3$  ratio increased (6.48, 6.67 and 6.83 by ICP), the  $\text{Na}_2\text{O}/\text{Al}_2\text{O}_3$  ratio decreased (0.72, 0.77 and 0.83 by ICP), and OSDA content raised accordingly (C %: 4.06%, 5.11% and 5.49% by elemental analysis). In the final liquid-solid mixture, a part of [choline] $^+$  and  $\text{Na}^+$  dissociate in the solution, and the other part of them fill in the micropores. There is inevitably a competition between  $\text{Na}^+$  and [choline] $^+$  acting as structure-directing agents and skeletal fillers in the synthesis of Y zeolite. The results demonstrate that the molar ratio of  $\text{Na}^+$  to [choline] $^+$  is a crucial factor for their competition and further

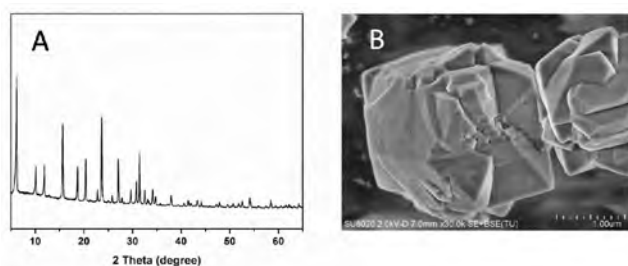


Fig. 4. XRD pattern (A) and SEM image (B) of ChCl/ChOH:0.5/0.5-Y.

influences the framework  $\text{SiO}_2/\text{Al}_2\text{O}_3$  ratio. The use of OSDAs in a  $\text{OH}^-$  form is a direct and efficient method to enhance the framework  $\text{SiO}_2/\text{Al}_2\text{O}_3$  ratio, which reduces the feedstock amount of  $\text{Na}^+$  to weaken the competitiveness of  $\text{Na}^+$ . However, when the feed of  $\text{Na}^+$  is reduced below 0.3, it is difficult to form uniform zeolite Y; the result accompanies lots of amorphous aluminosilicate (samples #1 and #2 in Table S2, Fig. S2 and Fig. S3). A certain amount of  $\text{Na}^+$  is an essential part of the synthesis of Y zeolite.

Normally, zeolite Y is synthesized at 100 °C with high alkalinity as the sample Na-Y. ChCl-Y and ChOH-Y are designed with low alkalinity at 110 °C because the low alkalinity and high crystallization temperature during the synthesis are helpful for enhancing the  $\text{SiO}_2/\text{Al}_2\text{O}_3$  ratio of the final zeolites. However, when the temperature is increased to 120 °C, the same aluminosilicate gel produces FAU and MAZ zeolite (samples #3 and #4 in Table S2, Fig. S4 and Fig. S5). When the feed molar fraction of choline cation is increased to 2.0, it is plainly a tendency that the final products transform from the FAU topology to MAZ structure (sample #5 in Table S2 and Fig. S6). Choline is also used as an OSDA for synthesizing zeolite ZSM-4 with MAZ framework [34].

### 3.3. Hydrothermal and thermal stability of ChCl-Y, ChOH-Y and Na-Y

It is well known that the (hydro)thermal stability of zeolite at high temperature has a strong relationship with the framework  $\text{SiO}_2/\text{Al}_2\text{O}_3$  ratio, which is a crucial factor for industrial applications. The exothermic peaks without weight variation above 800 °C in the TG/DSC curves are attributed to the structural collapse of zeolite Y, which is used as a main evaluation of the thermal stability of zeolites at high temperature. Na-Y starts to collapse at 970 °C (Fig. S7), but the skeleton of ChCl-Y and ChOH-Y remains stable until 1024 and 1030 °C (Fig. 2E and 2F). The results are also additional evidence that our materials have unusually ultrahigh  $\text{SiO}_2/\text{Al}_2\text{O}_3$  ratio. The crystallinity change before and after steam treatment at high temperature is a measure of the hydrothermal stability of zeolites. The XRD patterns of HChCl-Y, HChOH-Y and HNa-Y (the correspond H-form samples after ammonium ion exchange and calcination) before and after 100% steam treatment at 750 °C for 2 h are shown in Fig. 5. This indicates that the crystallinity of HNa-Y descends more steeply than that of HChCl-Y and HChOH-Y after steam treatment. The crystallinity of HChCl-Y and HChOH-Y retains 54.2% and 56.6%, higher than 38.5% of HNa-Y; BET specific surface area and *t*-plot micropore surface area of HNa-Y are obviously lower than that of HChCl-Y and HChOH-Y after steam treatment (Table 2). The results indicate that ChCl-Y and ChOH-Y exhibit a more superior hydrothermal and thermal stability owing to the higher framework  $\text{SiO}_2/\text{Al}_2\text{O}_3$  ratio. It is known that the bond energy of the silicon–oxygen bond (Si–O–Si) is higher than that of the aluminium–oxygen bond (Al–O–Si), so the Si–O–Si bond is more stable than the Al–O–Si bond. ChCl-Y and ChOH-Y have higher Si–O–Si/Al–O–Si ratio than Na-Y, which has been interpreted with the  $^{29}\text{Si}$ -NMR spectrum (Fig. 4). Collectively, these studies confirm the practical advantages of increasing Y zeolite  $\text{SiO}_2/\text{Al}_2\text{O}_3$  ratio to improve the (hydro)thermal stability, which enhances the adaptation of Y zeolite for catalytic applications.

## 4. Conclusions

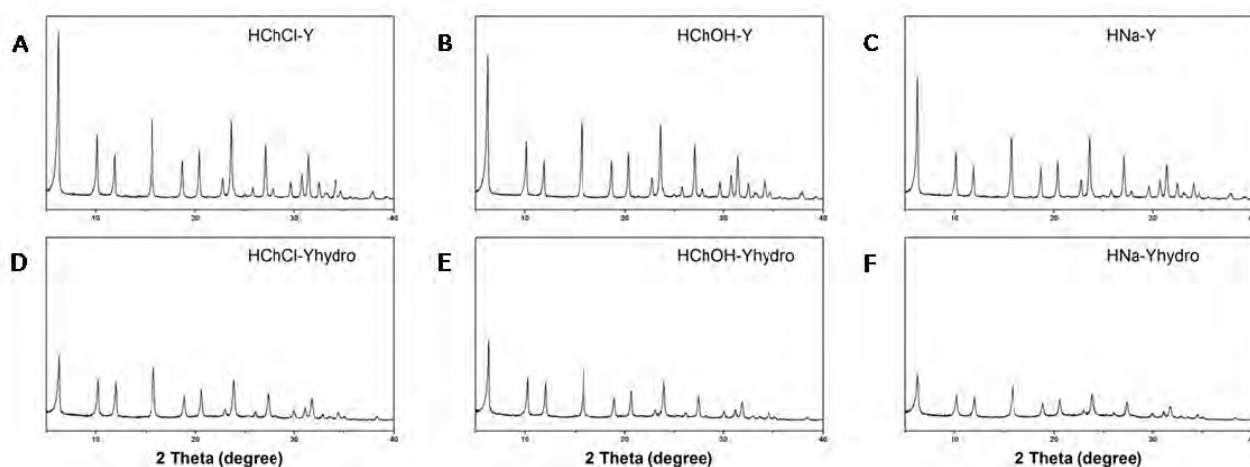


Fig. 5. XRD patterns of HChCl-Y (A), HChOH-Y (B), HNa-Y (C), HChCl-Yhydro (D), HChOH-Yhydro (E) and HNa-Yhydro (F). HChCl-Yhydro, HChOH-Yhydro and HNa-Yhydro are respectively corresponded to HChCl-Y, HChOH-Y and HNa-Y after 100% steam treatment at 750 °C for 2 h.

**Table 2**

Textural properties of HChCl-Y, HChOH-Y and HNaY samples before and after the hydrothermal treatment by 100% steam at 750 °C for 2 h.

Sample	Relative crystallinity <sup>a</sup> (%)	BET specific surface area (m <sup>2</sup> /g)	<i>t</i> -Plot micropore surface area (m <sup>2</sup> /g)	<i>t</i> -Plot external surface Area (cm <sup>3</sup> /g)
HChCl-Y	100	677.3	617.4	60.0
HChOH-Y	100	690.9	624.2	66.7
HNa-Y	100	535.4	490.8	44.6
HChCl-Yhydro	56.6	412.3	318.0	94.3
HChOH-Yhydro	54.2	507.5	418.6	88.9
HNa-Yhydro	38.5	352.4	302.1	50.0

<sup>a</sup> Estimated by the reflection intensities of the X-ray diffraction peaks (1 1 1), (2 2 0) and (3 3 1) of the samples.

A FAU zeolite with good crystallinity has been synthesized with the use of choline as an eco-friendly and biodegradable OSDA for the first time. The synthetic samples ChCl-Y and ChOH-Y have SiO<sub>2</sub>/Al<sub>2</sub>O<sub>3</sub> ratios of 6.48 and 6.83, which are much higher than that of common Y zeolite prepared by OSDA-free routes. Both ChCl-Y and ChOH-Y exhibit outstanding thermal and hydrothermal stability owing to higher SiO<sub>2</sub>/Al<sub>2</sub>O<sub>3</sub> ratio. Based on a thoughtful experiment design, it is proved that Na<sup>+</sup> show a seemingly stronger competitiveness than [choline]<sup>+</sup> in the cage of FAU zeolite and the feed fraction of Na<sup>+</sup> has a crucial influence on the FAU framework SiO<sub>2</sub>/Al<sub>2</sub>O<sub>3</sub> ratio. The use of OSDAs with OH<sup>-</sup> anion enhancing the zeolite SiO<sub>2</sub>/Al<sub>2</sub>O<sub>3</sub> ratio is a valued inspiration for the synthesis of high silica zeolite. These unique findings are of potential importance for the future industrial application of high silica FAU zeolite as an adsorbent and a catalyst.

## References

- [1] R. M. Barrer, *Zeolites*, **1981**, 1, 130–140.
- [2] M. E. Davis, R. F. Lobo, *Chem. Mater.*, **1992**, 4, 756–768.
- [3] M. E. Davis, *Nature*, **2002**, 417, 813–821.
- [4] A. Corma, *J. Catal.*, **2003**, 216, 298–312.
- [5] W. Vermeiren, J. P. Gilson, *Top. Catal.*, **2009**, 52, 1131–1161.
- [6] G. T. Kerr, G. T. Kokotailo, *J. Am. Chem. Soc.*, **1961**, 83, 4675.
- [7] C. S. Cundy, P. A. Cox, *Chem. Rev.*, **2003**, 103, 663–702.
- [8] L. A. Villaescusa, W. Zhou, R. E. Morris, P. A. Barrett, *J. Mater. Chem.*, **2004**, 14, 1982–1987.
- [9] X. Meng, F. S. Xiao, *Chem. Rev.*, **2014**, 114, 1521–1543.
- [10] L. Ren, L. Zhu, C. Yang, Y. Chen, Q. Sun, H. Zhang, C. Li, F. Nawaz, X. Meng, F. S. Xiao, *Chem. Commun.*, **2011**, 47, 9789–9791.
- [11] S. I. Zones, S. J. Hwang, *Chem. Mater.*, **2002**, 14, 313–320.
- [12] S. Liu, L. Li, C. Li, X. Xiong, F. S. Xiao, *J. Porous Mater.*, **2008**, 15, 295–301.
- [13] D. W. Breck, *US Patent*, 3130007A, **1964**.
- [14] P. K. Maher, E. W. Albers, C. V. McDaniel, *US Patent*, 3639099A, **1972**.
- [15] J. P. Arhancet, M. E. Davis, *Chem. Mater.*, **1991**, 3, 567–569.
- [16] S. M. Babitz, B. A. Williams, J. T. Miller, R. Q. Snurr, W. Q. Haag, H. H. Kung, *Appl. Catal., A*, **1999**, 179, 71–86.
- [17] M. A. Camblor, A. Corma, A. Martínez, F. A. Mocholí, J. P. Pariente, *Appl. Catal.*, **1989**, 55, 65–74.
- [18] E. F. S. Aguiar, M. L. M. Valle, M. P. Silva, D. F. Silva, *Zeolites*, **1995**, 15, 620–623.

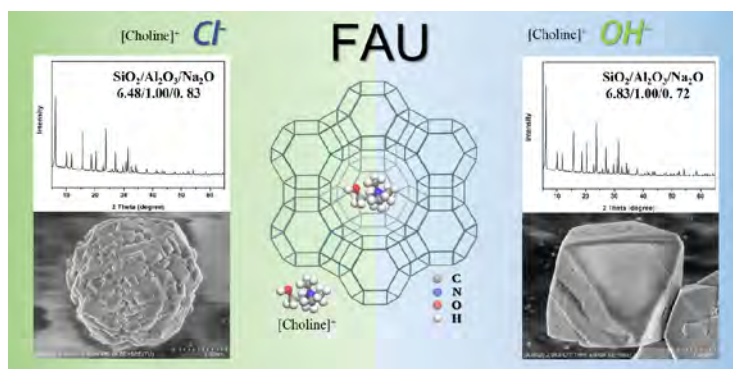
## Graphical Abstract

*Chin. J. Catal.*, 2019, 40: 52–59 doi: 10.1016/S1872-2067(18)63167-5

### Eco-friendly synthesis of high silica zeolite Y with choline as green and innocent structure-directing agent

Dawei He, Danhua Yuan, Zhijia Song, Yunpeng Xu\*, Zhongmin Liu\*

Dalian Institute of Chemical Physics, Chinese Academy of Sciences; University of Chinese Academy of Sciences



Choline chloride or choline hydroxide was used as an eco-friendly and nontoxic organic structure-directing agent (OSDA) for the synthesis of high silica zeolite Y with SiO<sub>2</sub>/Al<sub>2</sub>O<sub>3</sub> ratios of 6.5–6.8.



- [19] R. A. Beyerlein, G. B. McVicker, L. N. Yacullo, J. J. Ziemiak, *J. Phys. Chem.*, **1988**, 92, 1967–1970.
- [20] B. Xu, S. Bordiga, R. Prins, J. A. van Bokhoven, *Appl. Catal. A*, **2007**, 333, 245–253.
- [21] M. D. Oleksiak, K. Muraoka, M. F. Hsieh, M. T. Conato, A. Shimojima, T. Okubo, W. Chaikittisilp, J. D. Rimer, *Angew. Chem. Int. Ed.*, **2017**, 56, 13366–13371.
- [22] L. Kubelková, S. Beran, A. Malecka, V. M. Mastikhin, *Zeolites*, **1989**, 9, 12–17.
- [23] G. Garralon, V. Fornes, A. Corma, *Zeolites*, **1988**, 8, 268–272.
- [24] J. Datka, W. Kolidziejewski, J. Klinowski, B. Sulikowski, *Catal. Lett.*, **1993**, 19, 159–165.
- [25] E. F. T. Lee, L. V. C. Rees, *J. Chem. Soc., Faraday Trans. 1*, **1987**, 83, 1531–1537.
- [26] X. H. Du, X. L. Li, H. T. Zhang, X. H. Gao, *Chin. J. Catal.*, **2016**, 37, 316–323.
- [27] F. Delprato, L. Delmotte, J. L. Guth, L. Huve, *Zeolites*, **1990**, 10, 546–552.
- [28] F. Dognier, J. Patarin, J. L. Guth, D. Anglerot, *Zeolites*, **1993**, 13, 122–127.
- [29] L. Zhu, L. Ren, S. Zeng, C. Yang, H. Zhang, X. Meng, M. Rigutto, A. van der Made, F. S. Xiao, *Chem. Commun.*, **2013**, 49, 10495–10497.
- [30] D. Yuan, D. He, S. Xu, Z. Song, M. Zhang, Y. Wei, Y. He, S. Xu, Z. Liu, Y. Xu, *Microporous Mesoporous Mater.*, **2015**, 204, 1–7.
- [31] D. He, D. Yuan, Z. Song, Y. Tong, Y. Wu, S. Xu, Y. Xu, Z. Liu, *Chem. Commun.*, **2016**, 52, 12765–12768.
- [32] S. H. Zeisel, *Ann. Nutr. Metab.*, **2012**, 61, 254–258.
- [33] F. Liu, M. Audemar, K. De Oliveira Vigier, D. Cartigny, J. M. Clacens, M. F. C. Gomes, A. A. H. Padua, F. De Campo, F. Jerome, *Green Chem.*, **2013**, 15, 3205–3213.
- [34] A. J. Perrotta, C. Kibby, B. R. Mitchell, E. R. Tucci, *J. Catal.*, **1978**, 55, 240–249.
- [35] B. Chen, R. Xu, R. Zhang, N. Liu, *Environ. Sci. Technol.*, **2014**, 48, 13909–13916.
- [36] X. Zhao, H. Wang, C. Kang, Z. Sun, G. Li, X. Wang, *Microporous Mesoporous Mater.*, **2012**, 151, 501–505.
- [37] A. I. Lupulescu, J. D. Rimer, *Angew. Chem. Int. Ed.*, **2012**, 51, 3345–3349.
- [38] A. I. Lupulescu, M. Kumar, J. D. Rimer, *J. Am. Chem. Soc.*, **2013**, 135, 6608–6617.
- [39] A. Burton, *Catal. Rev.-Sci. Eng.*, **2018**, 60, 132–175.

## 以胆碱为绿色无毒有机结构导向剂合成高硅Y型分子筛

贺大威<sup>a,b,†</sup>, 袁丹华<sup>a,†</sup>, 宋智甲<sup>a,b</sup>, 徐云鹏<sup>a,\*</sup>, 刘中民<sup>a,#</sup>

<sup>a</sup>中国科学院大连化学物理研究所洁净能源国家实验室(筹), 甲醇制烯烃国家工程实验室, 辽宁大连116023

<sup>b</sup>中国科学院大学, 北京100049

**摘要:** 分子筛作为一类重要的无机多孔晶体材料, 由于其规整的孔道结构以及优异的酸性质等特点, 在催化剂、吸附剂和离子交换床等许多领域有着重要而广泛的应用. 而现代分子筛制备方法的发展主要得益于有机结构导向剂(OSDA)在分子筛合成中的广泛使用. 但是, 大部分OSDA都具有剧毒、价格昂贵、制备方法繁琐等缺点, 因而限制了其大规模应用. 高硅Y型分子筛的合成研究也面临同样的问题.

Y型分子筛具有十二元环孔口和三维孔道结构, 是目前催化裂化催化剂中的主要活性组分. 目前, 通过常规合成方法无法获得硅铝比大于6.0的Y型分子筛, 无法满足石油化工对其酸性的要求. 目前工业上主要通过后处理法得到高硅Y沸石, 但该方法繁杂的后处理过程、不均匀的化学分布、大量损失的结晶度以及严重的环境污染促使人们开发直接合成高硅Y型分子筛的新方法以替代后处理过程. 此外, 使用OSDA一步法合成的高硅铝比Y型分子筛具有优异的热和水热稳定性. 因此, 使用OSDA一步直接合成高硅Y型分子筛在材料合成和催化领域一直备受关注. 然而, 目前尚未见关于绿色OSDA用于高硅Y型分子筛合成的报道.

本研究首次将氢氧化胆碱或氯化胆碱作为一种新型、绿色、廉价的OSDA引入到高硅Y分子筛的合成凝胶体系, 成功合成了高结晶度且硅铝比大于6.0的高硅Y型分子筛. 实验详细考察了合成条件对硅铝比的影响, 并采用XRD, XRF, NMR, TG以及N<sub>2</sub>物理吸附等表征手段研究了合成样品的物理化学性质. 表征结果证明, 胆碱阳离子作为一个稳定的OSDA存在于分子筛的孔结构中, 并且取代了部分Na<sup>+</sup>以平衡分子筛骨架的负电荷, 因此胆碱的使用可使样品的硅铝比提高并具有更加优异的热稳定性和水热稳定性. 实验确定了Na<sup>+</sup>和OSDA<sup>+</sup>在高硅Y分子筛合成中的竞争关系. 大量的实验证据表明, Na<sup>+</sup>的进料比例对FAU骨架硅铝比有决定性的影响. 首次提出采用氢氧根离子型OSDA是一种直接有效提高骨架硅铝比的方法.

**关键词:** 分子筛合成; FAU分子筛; 高硅铝比; 绿色有机结构导向剂; (水)热稳定性

收稿日期: 2018-09-12. 接受日期: 2018-09-23. 出版日期: 2019-01-05.

<sup>†</sup>共同第一作者.

\*通讯联系人. 电话: (0411)84379518; 传真: (0411)84379038; 电子邮箱: xuy@dicp.ac.cn

#通讯联系人. 电话: (0411)84379998; 传真: (0411)84379038; 电子邮箱: liuzm@dicp.ac.cn

本文的电子版全文由Elsevier出版社在ScienceDirect上出版(<http://www.sciencedirect.com/science/journal/18722067>).